Approximate Nonlinear Slender Wing Aerodynamics

Lars E. Ericsson* and J. Peter Reding†
Lockheed Missiles & Space Company, Inc., Sunnyvale, Calif.

On present-day high-performance aircraft, a large portion of the lift at moderate to high angles of attack is produced by leading-edge vortices, generated by flow separation off the highly swept leading edges of the lifting surfaces employed. It has been shown in an earlier paper how the vortex effects can be superimposed on a modified slender wing theory to give the unsteady longitudinal characteristics of sharp-edged delta wings up to very high angles of attack. The present paper extends the previous analysis to include the effects of leading-edge roundness and trailing-edge sweep on the aerodynamic characteristics. The paper also derives analytic means for prediction of the yaw stability of slender wings and the first-order effects of Mach number. Universal scaling laws are defined for rapid preliminary design estimates of the slender wing lift and rolling moment.

Nomenclature

A = aspect ratio, $A = b^2/S$
b = wingspan
$\bar{c}$ = reference length (mean aerodynamic chord, for a delta wing $\bar{c} = 2c_0/3$)
c_0 = slender wing root chord
f_1, f_2 = functions defined in Eqs. (4, 5) and (28, 29), respectively
K_P, K_V = potential flow and vortex lift factors, Eq. (1)
K_{PI} = first approximation of K_P
L = lift: coefficient $C_L = L/(\rho_\infty U_\infty^2/2)S$
l = rolling moment: coefficient $C_l = l/(\rho_\infty U_\infty^2/2)Sb$
M = Mach number
M_p = pitching moment: coefficient $C_m = M_p/(\rho_\infty U_\infty^2/2)S\bar{c}$
N = normal force: coefficient $C_N = N/(\rho_\infty U_\infty^2/2)S$
q = pitch rate
r_N = airfoil nose radius
Re = Reynolds number
S = reference area (= projected wing area)
S_{TE} = inefficient wing area at $M_\infty = 0$ (see inset in Fig. 1)
s = local semispan
t = time
U = horizontal velocity
x, y = body-fixed coordinates (see inset in Fig. 1)
α = angle of attack
α_0 = trim angle of attack
β = sideslip angle (see inset in Fig. 4)
η = dimensionless y coordinate, $\eta = y/s$
$\bar{\eta}$ = center of pressure location
θ = pitch perturbation around α_0
θ_{LE} = apex half-angle (see inset in Fig. 1)
θ_{TE} = trailing-edge sweep angle (Fig. 9)
μ = Mach angle, $\mu = \text{cosec}^{-1}(M_\infty)$
ξ = dimensionless x coordinate, $\xi = x/c_0$
$\bar{\xi}$ = center of pressure location
ρ = air density
$\omega, \bar{\omega}$ = pitching frequency, $\bar{\omega} = \omega c_0/U_\infty$

Subscripts

a = attached flow
CG = center of gravity or pitch axis location
eff. = effective
LE = leading edge
max = maximum
N or $\perp$ = normal to leading edge
s = separated flow
TE = trailing edge
V = vortex
2D = two-dimensional flow
∞ = freestream conditions

Superscripts

(*) = trailing-edge parameters, Eq. (36)

Derivative Symbols

$\dot{\theta}$ = $\partial\theta/\partial t$
$C_{L\alpha}$ = $\partial C_L/\partial\alpha$; $C_{l\beta} = \partial C_l/\partial\beta$; $C_{m\theta} = \partial C_m/\partial\theta$
$C_{mq} + C_{m\dot{\alpha}}$ = $\partial C_m/\partial(\bar{c}q/U_\infty) + \partial C_m/\partial(\bar{c}\dot{\alpha}/U_\infty)$

Introduction

THE complexity of the flowfield on aircraft or aircraftlike configurations that operate at high angles of attack prohibit the use of purely theoretical means. Because of the continual changes in the early design, a purely experimental approach cannot be used either. One needs theoretical means that permit analytic extrapolation from experimental data, similar to those developed for the Saturn-Apollo launch vehicle.[1,2] One example of an advanced aircraftlike configuration is the space shuttle orbiter. As it has basically a delta wing planform, analytic means are needed for the prediction of the unsteady delta wing aerodynamics, including the effects of the leading-edge vortices generated at nonzero angle of attack. Such a theory, described in Ref. 3, is valid for the symmetric unsteady aerodynamic characteristics of sharp-edged delta wings in incompressible flow. The present paper describes how this theory can be extended to include the effects of trailing-edge sweep and leading-edge roundness. Simple analytic means are also derived for computation of the static stability in yaw and first-order Mach number effects. Correlation formulas for preliminary design estimates are given for the nonlinear slender wing lift and the rolling moment sideslip derivative.

Analysis

The slender wing lift can be determined as follows for a sharp-edged delta wing[4]:

$$C_L = K_p \sin\alpha \cos 2\alpha + K_V \sin^2\alpha \cos\alpha \qquad (1)$$

Presented as Paper 76-19 at the AIAA 14th Aerospace Sciences Meeting, Washington, D.C., Jan. 26-28, 1976; submitted Aug. 11, 1976; revision received May 10, 1977.
Index category: Nonsteady Aerodynamics.
*Consulting Engineer. Associate Fellow AIAA.
†Research Specialist. Member AIAA.

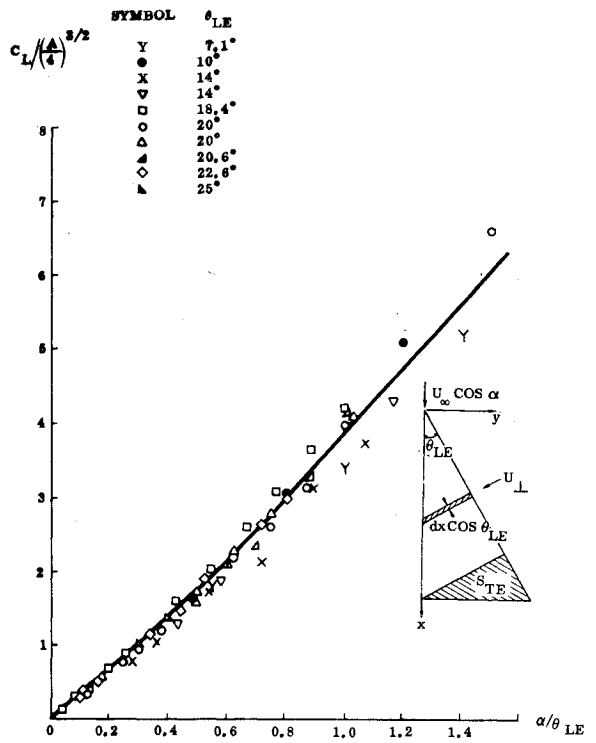

Fig. 1 Universal scaling of delta wing lift.

K_P and K_V are constants determining the magnitudes of attached flow and vortex lift components, respectively. K_V is for all practical purposes a true constant,[4] whereas K_P is more or less linearly dependent upon aspect ratio. A first approximation of K_P is obtained as follows.[3] It is assumed that the area denoted S_{TE} in the inset of Fig. 1 carries no load. This accounts in a crude manner for the trailing-edge condition at $M_\infty = 0$ (as compared to $M_\infty = 1$). It reduces Jones' slender wing lift[5] by the factor $\cos^2\theta_{LE}$ giving

$$K_{PI} = \frac{\pi(A/2)}{1+(A/4)^2} \tag{2}$$

With $C_L = C_N \cos\alpha$ and $K_V = \pi$, Eqs. (1) and (2) give the following definition of the total delta wing lift:

$$\frac{C_L}{(A/4)^2} = 2\pi\cos^3\alpha\left\{\left(\frac{\tan\alpha}{\tan\theta_{LE}}\right)\times\left[\left(1+\left(\frac{A}{4}\right)^2\right]^{-1}+\frac{1}{2}\left(\frac{\tan\alpha}{\tan\theta_{LE}}\right)^2\right]\right\} \tag{3}$$

Equation (3) shows that $(\tan\alpha/\tan\theta_{LE}) \approx \alpha/\theta_{LE}$ is the pertinent scaling parameter for angle-of-attack effects. However, the appearance of $A/4$ inside the bracket on the right-hand side of Eq. (3) invalidates the usefulness of $(A/4)^2$ as the normalizing unit for the lift. Hence, another procedure was sought to represent the total delta wing lift. Following Peckham's suggestion[6] the exponent 3/2 was selected instead of 2, and available experimental data for sharp-edged delta wings were plotted in form of

$$C_L(A/4)^{-3/2} = f_1(\alpha/\theta_{LE}) \tag{4}$$

The result, shown in Fig. 1, speaks for itself. The experimental data[6-11] collapse into one (preliminary design) curve. Thus, for preliminary design purposes the nonlinear delta wing lift is determined from Fig. 1 to be

$$C_L(A/4)^{-3/2} = 3.4(\alpha/\theta_{LE}) + 0.45(\alpha/\theta_{LE})^2 \tag{5}$$

It was shown in Ref. 3 that the potential flow loading on a delta wing never exceeded 75% of the maximum given by slender wing theory. Applying this "ceiling" gives[3]

$$C_{Na} = 0.91K_{PI}\sin\alpha\cos\alpha \tag{6a}$$

$$C_{ma} = -(c_0/\bar{c})C_{Na}(\bar{\xi}_a - \xi_{CG}) \tag{6b}$$

$$\bar{\xi}_a = 0.64(1-\Delta\xi_{aTE}) \tag{6c}$$

$$\Delta\xi_{aTE} = \bar{\eta}_a\sin^2\theta_{LE} \quad (\bar{\eta}_a = 4/3\pi, \text{ elliptic loading}) \tag{6d}$$

It was also demonstrated in Ref. 3 that the vortex-induced load distribution on a sharp-edged delta wing does not have the triangular shape prescribed by the conic flow assumption used in most theories, but has a "ceiling" similar to that of the attached flow. The resulting load distribution for the 70% of the vortex-induced loading located near the leading edge is

$$\frac{1}{0.7}\frac{1}{2}\left(\frac{dC_{NV}}{d\xi}\right)_\perp = \begin{cases} 1.75\pi\xi\sin^2\alpha & (\xi \le 0.4) \\ 0.685\pi\sin^2\alpha & (0.4 < \xi < 0.9) \\ 6.85\pi\sin^2\alpha(1-\xi) & (0.9 \le \xi \le 1.0) \end{cases} \tag{7}$$

and the distribution of the remaining 30% loading produced by the vortex entrainment is

$$\frac{1}{0.3}\frac{1}{2}\left(\frac{dC_{NV}}{d\xi}\right)_\perp = \begin{cases} 1.05\pi\xi\sin^2\alpha & (\xi \le 0.7) \\ 0.735\pi\sin^2\alpha & (0.7 < \xi \le 1.0) \end{cases} \tag{8}$$

Integration of Eqs. (7) and (8) gives:

$$C_{NV} = \pi\sin^2\alpha \tag{9a}$$

$$C_{mV} = -(c_0/\bar{c})C_{NV}[0.7(\bar{\xi}_V - \xi_{CG}) + 0.3(\bar{\xi}_a - \xi_{CG})] \tag{9b}$$

$$\bar{\xi}_V = 0.56(1-\bar{\eta}_V\sin^2\theta_{LE}) \tag{9c}$$

$$\bar{\xi}_a = 0.64(1-\bar{\eta}_a\sin^2\theta_{LE}) \tag{9d}$$

$\bar{\eta}_a = 4/3\pi$, and $\bar{\eta}_v$, given by experimental data,[12] is $\bar{\eta}_v = 0.56 + 0.36/[1.75 + (\alpha/\theta_{LE})]$.

It was shown in Ref. 3 how the unsteady aerodynamics for the attached flow loads could be determined by using slender wing theory[5] on an equivalent delta wing which has been shortened to provide the correct normal force. The effective center chord for this equivalent wing is[3]

$$c_{eff}/c_0 = 0.955\cos\theta_{LE}(2-\cos^{-2}\alpha_0)^{1/2} \tag{10}$$

The center of pressure is obtained as follows for moderate α_0, $(\cos\alpha_0 \approx 1)$.

$$\tfrac{2}{3}c_{eff}/c_0 = 0.64(1-\tfrac{1}{2}\sin^2\theta_{LE}+\ldots) \tag{11}$$

This compares well with the value given by Eq. (6), $\bar{\xi}_a = 0.64(1-0.425\sin^2\theta_{LE})$, at least for slender wings, $\sin^2\theta_{LE} \ll 1$.

The capacity of the foregoing simple analysis to predict the experimentally measured low-speed unsteady aerodynamics of delta wings up to high angles of attack was demonstrated in Ref. 3, and will not be elaborated on here. Instead, it will be outlined how the analysis has been extended to include the effects of trailing-edge sweep, leading-edge roundness, and compressibility.

Effect of Leading-Edge Roundness

Gersten[13] has shown that leading-edge roundness has a large effect on delta wing aerodynamics (Fig. 2). A large part

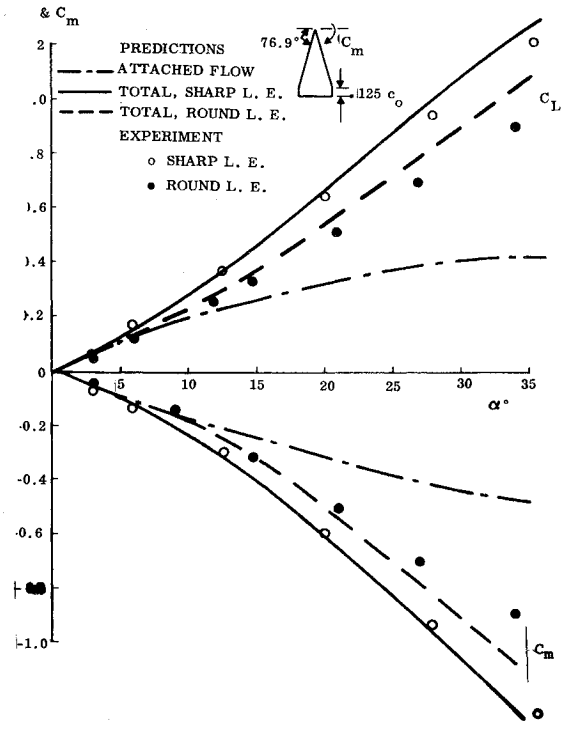

Fig. 2 Comparison of predicted and measured effects of leading-edge roundness on static characteristics of a slender wing of aspect ratio $A = 0.78$.

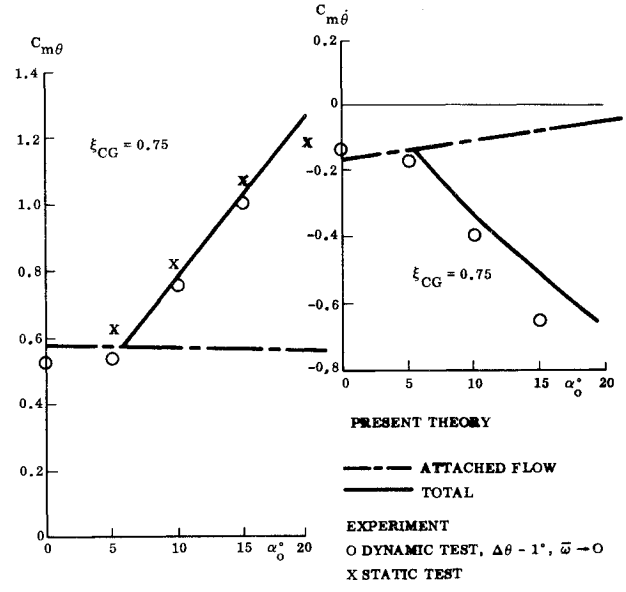

Fig. 3 Comparison between predicted and measured dynamic stability characteristics of an $A = 1.484$ delta wing with rounded leading edge.

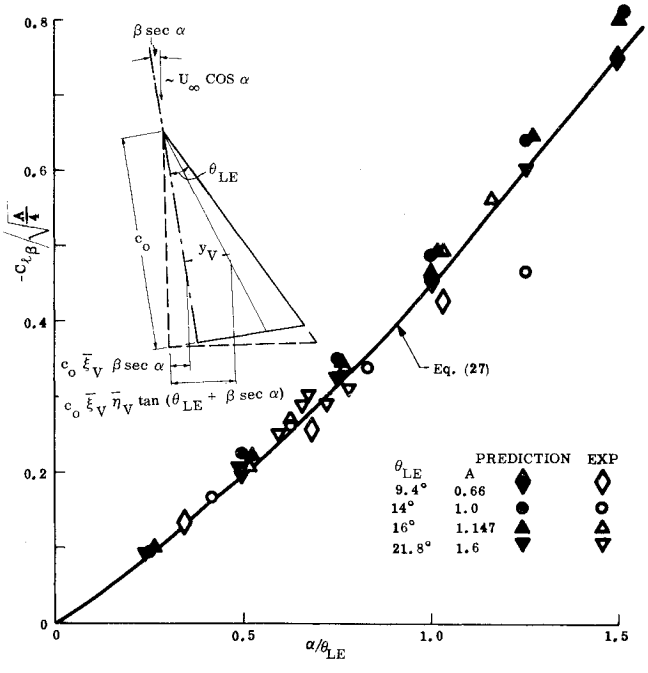

Fig. 4 Universal scaling of delta wing sideslip derivative $C_{l\beta}$ at $\beta = 0$.

of the measured decrease in lift and statically stabilizing pitching moment is probably due to roundness-induced delay of the leading-edge separation and associated delay of the vortex lift generation.‡ According to Ville,[15] leading-edge separation should, in two-dimensional flow, occur at an angle of attack α_{2Ds} that is determined by profile nose radius and freestream Reynolds number. It is clear that the three-dimensional flow will delay the separation in the crossflow plane to an angle of attack $\alpha_{Ns} > \alpha_{2Ds}$. An estimate of this delay is obtained by defining an effective aspect ratio $A_N = 4c_0/b$ for half§ the delta wing in the crossflow plane. Assuming that $C_{L\max}$ is independent of aspect ratio one obtains[16]

$$\alpha_{Ns}/\alpha_{2Ds} = 1 + 2/A_N = (1 + \tan\theta_{LE}) \tag{12}$$

For the small angles of attack of interest the streamwise angle of attack α_s is simply

$$\alpha_s = \alpha_{2Ds}(1 + \tan\theta_{LE})\sin\theta_{LE} \tag{13}$$

Experimental results[17] indicate that leading-edge stall on the NACA-0012 airfoil will occur in the angle-of-attack range 12.5 deg $\leq \alpha_{2Ds} \leq 18$ deg depending upon the Reynolds number. The test conditions for Gersten's data[13] suggest a value of $\alpha_{2Ds} = 13$ deg giving $\alpha_s = 3.95$ deg. Substituting $(\alpha - \alpha_s)$ for α in Eq. (9) gives the rounded leading-edge effect shown by the difference between the dashed and solid line curves in Fig. 2. Although the predicted effect of leading-edge roundness is in the right direction, it is less than what was observed experimentally. It was discussed in Ref. 3 how a slackening of the vortex-induced load buildup was observed to occur aft of 40% center chord ($\xi > 0.4$). This could be caused by a "loosening" of the vortex shedding; i.e., the vortex becomes less concentrated. Such an increase of the vortex core could occur for two possible reasons: 1) the center core axial velocity is decreasing or 2) the vortex shedding mechanism from the leading edge has changed. If the second reason is the significant one, the leading-edge roundness could be expected to contribute to further "loosening" of the vortex shedding with associated loss in vortex-induced lift. However, if the first reason dominates, which would be in accordance with one causative mechanism for vortex burst,[18,19] the leading-edge roundness effect should be accounted for by the $(\alpha - \alpha_s)$ correction. This appears to be the case judging by the good agreement between predictions and experimental dynamic results[20] for a delta wing with a rounded leading edge¶ (Fig. 3).

‡The 12.5% truncation of the wingtip (see sketch in Fig. 2) has no effect on the delta wing lift at $M_\infty = 0$ according to the present mathematical model (see sketch in Fig. 1). Recent results by Lamar[14] also indicate that the effect should be negligibly small.

§The leading-edge flow is insensitive to what happens on the other wing half.

¶For the 6% thick wing $\alpha_{2Ds} = 12$ deg, giving $\alpha_s = 5.7$ deg.

That this purely static effect of leading-edge roundness suffices to explain also the dynamic data is somewhat surprising in view of the large overshoot of static stall observed in dynamic testing of airfoils.[21] This is, however, in agreement with the dominance of flow conditions at the apex shown by Lambourne[22] for the unsteady vortex-induced load.[3]

Lateral Stability

The dominant lateral stability characteristic for a sideslipping delta wing is the rolling moment derivative $C_{l\beta}$. The analysis of Ref. 3 can be used as a basis to derive simple analytic relationships for the determination of $C_{l\beta}$. At an angle of sideslip (see inset in Fig. 4 for definitions) the effective apex angle of the windward side is increased by an amount $\Delta\theta_{LE}$ which is

$$\Delta\theta_{LE} = \tan^{-1}(\tan\beta/\cos\alpha) \tag{14}$$

or for small sideslip angles,

$$\Delta\theta_{LE} = \beta\sec\alpha \tag{15}$$

For attached flow the windward side normal force is increased because of the increased aspect ratio. Equations (1) and (2) give

$$C_N \sim K_P \qquad K_P = 2\pi\tan\theta_{LE}\cos^2\theta_{LE} \tag{16}$$

Thus, the β derivative for the normal force of the windward half of the delta wing can be determined as follows:

$$\frac{1}{2}\frac{1}{C_{Na}}\frac{dC_{Na}}{d\beta} = \frac{1}{2}\frac{1}{K_P}\frac{\partial K_P}{\partial\theta_{LE}}\frac{d\theta_{LE}}{d\beta} \tag{17a}$$

$$\frac{1}{K_P}\frac{\partial K_P}{\partial\theta_{LE}} = \cot\theta_{LE} - \tan\theta_{LE} \tag{17b}$$

$$\frac{d\theta_{LE}}{d\beta} = \sec\alpha \tag{17c}$$

The corresponding rolling moment derivative for the wing half is

$$-\frac{1}{2}\frac{dC_{la}}{d\beta} = \frac{1}{2}\frac{dC_{Na}}{d\beta}\frac{\bar{y}_a}{b} \qquad \frac{\bar{y}_a}{b} = \frac{\bar{\xi}_a\bar{\eta}_a}{2} \tag{18}$$

and the derivative for the full delta wing becomes

$$-\frac{dC_{la}}{d\beta} = \frac{\bar{\xi}_a\bar{\eta}_a}{2}\frac{C_{Na}}{\cos\alpha}(\cot\theta_{LE} - \tan\theta_{LE}) \tag{19}$$

For the attached flow loads, the load distribution remains the same for small sideslip angles. This is not true for the vortex-induced loads, which are determined only by the conditions at the leading edge. The loads given by Eq. (7) are the same regardless of whether it is a swept wing or a delta wing. That is, the presence of the center wing area of the delta wing has no effect on the vortex strength and the vortex-induced loads near the leading edge, given by Eq. (7). It is only needed to realize the vortex entrainment effect, Eq. (8). Thus, the windward half of the delta wing has the following increased load due to the sideslip angle (see inset in Fig. 4).

$$\tfrac{1}{2}C_{NV}(\alpha,\beta) = \tfrac{1}{2}C_{NV}(\alpha,0)\,S(\alpha,\beta)/S(\alpha,0) \tag{20a}$$

$$S(\alpha,\beta)/S(\alpha,0) = 1 + \beta\sec\alpha(\cot\theta_{LE} - \tan\theta_{LE}) \tag{20b}$$

That is

$$\frac{1}{2}\left(\frac{dC_{NV}}{d\beta}\right)_{\beta=0} = \frac{C_{NV}}{2\cos\alpha}(\cot\theta_{LE} - \tan\theta_{LE}) \tag{21}$$

For the 70% of the vortex-induced load located near the leading edge, Eq. (8), the effective lever arm $\bar{y}_V$ for the rolling moment is (see inset in Fig. 4)

$$\bar{y}_V = \bar{\xi}_V c_0[\bar{\eta}_V(\tan\theta_{LE} + \beta\sec\alpha) - \beta\sec\alpha]\cos(\beta\sec\alpha) \tag{22}$$

For small sideslip angles β the effective dimensionless lever arm for the windward half of the delta wing is

$$\left(\frac{\bar{y}_V}{b}\right)_{0.7} = \frac{\bar{\xi}_V\bar{\eta}_V}{2}\left[1 - \left(\frac{1-\bar{\eta}_V}{\bar{\eta}_V}\right)\left(\frac{\beta\cot\theta_{LE}}{\cos\alpha}\right)\right] \tag{23}$$

For the 30% of the vortex load caused by entrainment effects the dimensionless lever arm is

$$\left(\frac{\bar{y}_V}{b}\right)_{0.3} = \frac{\bar{\xi}_a\bar{\eta}_a}{2} \tag{24}$$

The β derivative of the rolling moment for the windward half of the delta wing is

$$-\frac{1}{2}\left(\frac{dC_{lV}}{d\beta}\right) = \frac{0.7}{2}\frac{\partial C_{NV}}{\partial\beta}\left(\frac{\bar{y}_V}{b}\right)_{0.7} + \frac{0.7}{2}C_{NV}\frac{\partial}{\partial\beta}\left(\frac{\bar{y}_V}{b}\right)_{0.7} + \frac{0.3}{2}\frac{\partial C_{NV}}{\partial\beta}\left(\frac{\bar{y}_V}{b}\right)_{0.3} \tag{25}$$

Equations (21-25) define the following rolling moment derivative for the vortex-induced loads on a delta wing

$$-\left(\frac{dC_{lV}}{d\beta}\right)_{\beta=0} = \frac{C_{NV}}{2\cos\alpha}\cot\theta_{LE}\{0.7\bar{\xi}_V[(2-\tan^2\theta_{LE})\bar{\eta}_V - 1] + 0.3\bar{\xi}_a(1-\tan^2\theta_{LE})\bar{\eta}_a\} \tag{26}$$

The dependence of $C_{l\beta}$ on $C_L(=C_N\cos\alpha)$ and θ_{LE}, together with the $C_L(\alpha/\theta_{LE})$-correction shown earlier (Fig. 1), strongly suggests that it should be possible to develop a scaling law also for $C_{l\beta}$. From Eqs. (19) and (26) one concludes that for moderate angles of attack (α) and small apex angles (θ_{LE}) the following should hold true

$$-\frac{C_{l\beta}}{[C_L(A/4)^{-1}]} = \text{constant} \tag{27}$$

From Eq. (3), $C_L(A/4)^{-3/2} = f_1(\alpha/\theta_{LE})$ and Eq. (27) becomes

$$-C_{l\beta}(A/4)^{-1/2} = f_2(\alpha/\theta_{LE}) \tag{28}$$

Figure 4 indicates that Eq. (18) is valid for aspect ratios $A \le 1.6$ and shows also that present predictions for delta wings agree well with experimental low-speed results.[23-26]

For moderate angles of attack Fig. 4 gives the following preliminary design estimate of $C_{l\beta}$ for delta wings. (How trailing-edge sweep can be accounted for will be described later.)

$$-C_{l\beta}(A/4)^{-1/2} = 0.35(\alpha/\theta_{LE}) + 0.10(\alpha/\theta_{LE})^2 \tag{29}$$

The roll stability derivative given by Eqs. (19) and (26) in combination with Eqs. (6) and (9) is in excellent agreement with experimental data[23] (Fig. 5).

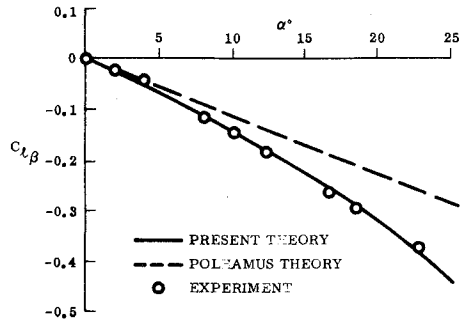

Fig. 5 Comparison between predicted and measured yaw stability derivatives.

Mach Number Effects

At sonic speed Jones' slender wing theory[5] applies. Thus, the whole wing is effective i.e., $S_{TE}=0$ and the "plateauing" does not occur. The attached load distribution along the center chord is as follows for $M_\infty=1$:

$$\frac{1}{2}\frac{dC_{Na}}{d\xi}=\frac{\pi\sin 2\alpha\tan^2\theta_{LE}}{A/4}\xi \qquad (0\le\xi\le 1.0) \tag{30}$$

The corresponding vortex-induced load distribution is

$$\frac{1}{0.7}\frac{1}{2}\frac{dC_{NV}}{d\xi}=\begin{cases}1.75\pi\xi\sin^2\alpha & (0\le\xi\le 0.4)\\ 0.685\pi\sin^2\alpha & (0.4<\xi\le 1.0)\end{cases} \tag{31a}$$

$$\frac{1}{0.3}\frac{1}{2}\frac{dC_{NV}}{d\xi}=1.05\pi\xi\sin^2\alpha \qquad (0\le\xi\le 1.0) \tag{31b}$$

Integration gives the following aerodynamic characteristics of a delta wing at $M_\infty=1.0$:

$$C_{Na}=\pi(A/2)\sin\alpha\cos\alpha \tag{32a}$$

$$C_{ma}=-(c_0/\bar{c})C_{Na}(\bar{\xi}_a-\xi_{CG}) \tag{32b}$$

$$C_{NV}=\pi\sin^2\alpha\sec^2\theta_{LE} \tag{32c}$$

$$C_{mv}=-(c_0/\bar{c})C_{NV}[0.3(\bar{\xi}_a-\xi_{CG})+0.7(\bar{\xi}_V-\xi_{CG})] \tag{32d}$$

$$\bar{\xi}_a=0.667 \qquad \bar{\xi}_V=0.587 \tag{32e}$$

An obvious way to make a smooth transition from $M_\infty=0$ to $M_\infty=1.0$ in regard to S_{TE} is the following:

$$S_{TE}(M_\infty)=S_{TE}(0)=0\sqrt{1-M_\infty^2} \tag{33}$$

Applying the same smoothening also to the load distribution gives the following unified representation of the subsonic longitudinal aerodynamic characteristics of a delta wing.

$$C_{Na}=\pi(A/2)\sin\alpha\cos\alpha(1-0.09\sqrt{1-M_\infty^2}\times(1-\sin^2\theta_{LE}\sqrt{1-M_\infty^2}) \tag{34a}$$

$$C_{ma}=-(c_0/\bar{c})C_{Na}(\bar{\xi}_a-\xi_{CG}) \tag{34b}$$

$$C_{NV}=\pi\sin^2\alpha\sec^2\theta_{LE}(1-\sin^2\theta_{LE}\sqrt{1-M_\infty^2}) \tag{34c}$$

$$C_{mV}=-(c_0/\bar{c})C_{NV}[0.3(\bar{\xi}_a-\xi_{CG})+0.7(\bar{\xi}_V-\xi_{CG})] \tag{34d}$$

$$\bar{\xi}_a=(0.667-0.027\sqrt{1-M_\infty^2})(1-\bar{\eta}_a\sin^2\theta_{LE}\sqrt{1-M_\infty^2}) \tag{34e}$$

$$\bar{\xi}_V=(0.587-0.027\sqrt{1-M_\infty^2})(1-\bar{\eta}_V\sin^2\theta_{LE}\sqrt{1-M_\infty^2}) \tag{34f}$$

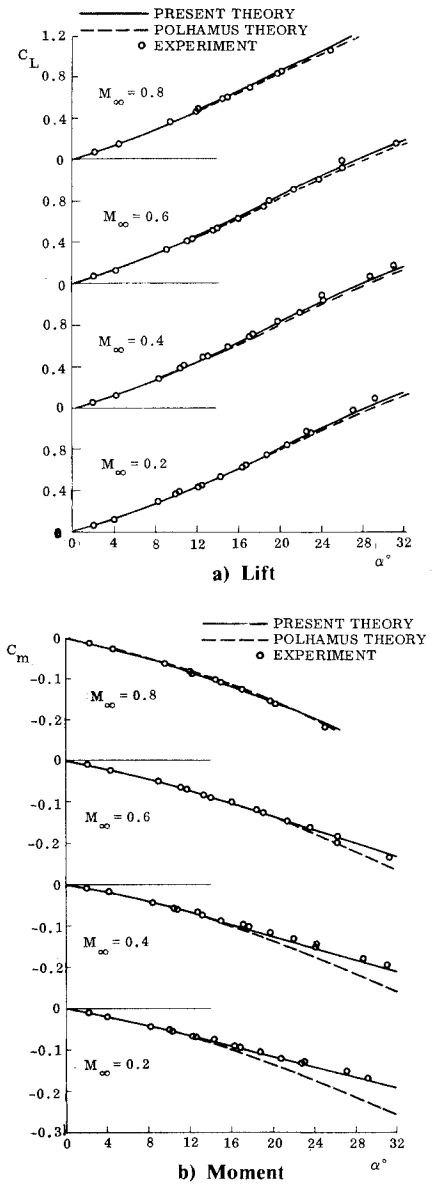

Fig. 6 Effect of subsonic Mach number on longitudinal delta wing aerodynamics.

For determination of the unsteady aerodynamics[3] Eq. (10) should be substituted by

$$c_{eff.}/c_0=[(1-0.09\sqrt{1-M_\infty^2})(1-\sin^2\theta_{LE}\times\sqrt{1-M_\infty^2})(2-\cos^{-2}\alpha_0)]^{1/2} \tag{35}$$

$C_{N\alpha V}$, $\bar{\xi}_a$, and $\bar{\xi}_V$ are obtained from Eq. (34). The expressions for the rolling moment derivative remain the same as before, Eqs. (19) and (26). Figure 6 shows that the longitudinal aerodynamic characteristics of a delta wing at subsonic speeds predicted by Eq. (34) are in excellent agreement with experimental data.[23] Combining Eq. (34) with Eqs. (19) and (26) gives predicted rolling moment derivatives at $\beta=0$ that also are in good agreement with the experimental results[23] (Fig. 7).

Effect of Trailing-Edge Sweep

The delta wing analysis can be extended to apply to slender wings with moderately swept leading and trailing edges. Two equivalent delta wings are defined, one for the attached flow loads and another for the vortex-induced loading (see Fig. 8). The equivalent delta wing characteristics are referenced to the

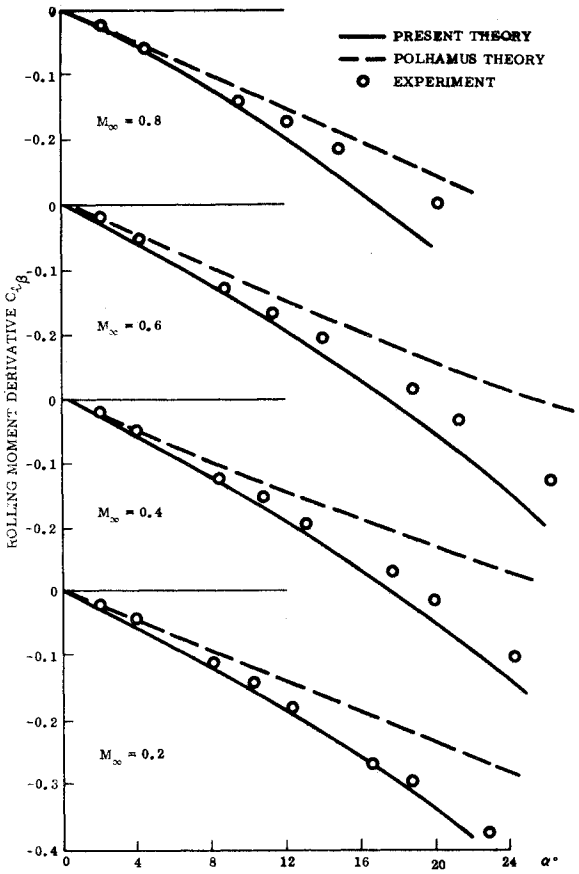

Fig. 7 Effect of subsonic Mach number on lateral delta wing characteristics.

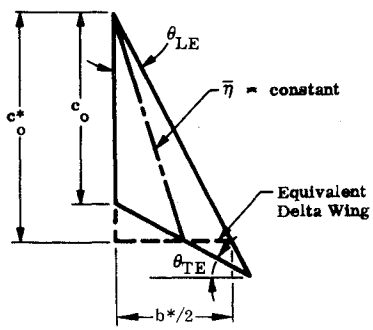

Fig. 8 Definition of trailing-edge parameters.

slender wing geometry using the following ratios (the asterisk indicates parameter values for the equivalent delta wing):

$$S^*/S = (1-\tan\theta_{LE}\tan\theta_{TE})/(1-\bar{\eta}\tan\theta_{LE}\tan\theta_{TE})^2 \quad (36a)$$

$$c^*_0/c_0 = 1/(1-\bar{\eta}\tan\theta_{LE}\tan\theta_{TE}) \quad (36b)$$

$$b^*/b = (1-\tan\theta_{LE}\tan\theta_{TE})/(1-\bar{\eta}\tan\theta_{LE}\tan\theta_{TE}) \quad (36c)$$

Figures 9 and 10 show that the low-speed longitudinal and lateral stability characteristics predicted by use of Eq. (36) in combination with the delta wing expressions [Eqs. (6, 9, 19, and 26)] agree well with experimental results.[23] It is apparent that the present method offers a definite improvement over the Polhamus theory,[4] especially in regard to the arrow wing characteristics. This is true also at high subsonic speed, $M_\infty = 0.8$ (Figs. 11 and 12).

Conclusions

The earlier developed analytic theory for the unsteady aerodynamics of delta wings at high angles of attack has been

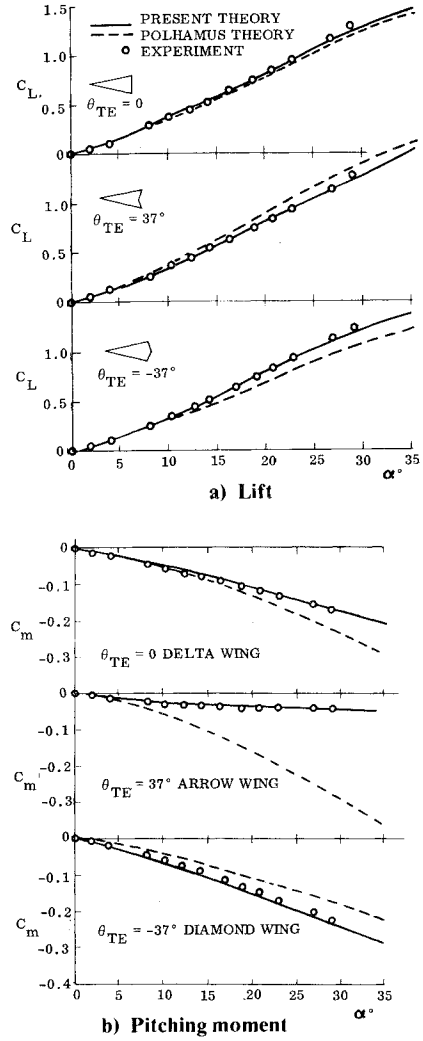

Fig. 9 Effect of trailing-edge sweep on longitudinal aerodynamics at $M_\infty = 0.2$.

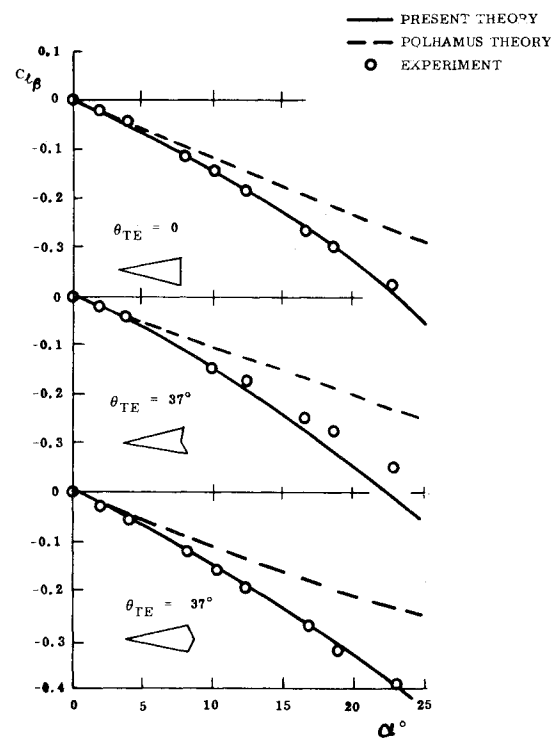

Fig. 10 Effect of trailing-edge sweep on lateral stability at $M_\infty = 0.2$.

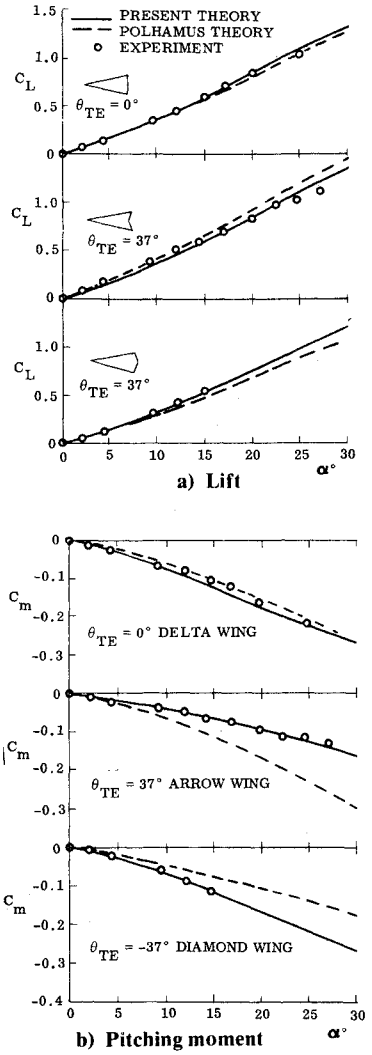

Fig. 11 Effect of trailing-edge sweep on longitudinal aerodynamics at $M_\infty = 0.8$.

extended to more general slender wing geometries, giving the following results:

1) The effect of Mach number for a subsonic leading edge is accounted for by a simple modification of Jones' slender wing theory for the attached flow loads and by a reformulation of Polhamus' theory for the vortex loads.

2) The effect of leading-edge roundness can be predicted by considering the delay of leading-edge separation in the crossflow plane generated by the rounded leading edge.

3) The effect of trailing-edge sweep (forward or back) is well predicted by use of two equivalent delta wings, one for the attached flow loads and another for the vortex loads.

4) Both longitudinal and lateral stability derivatives can be determined with good accuracy by the presented closed-form solutions.

5) Universal scaling concepts have been developed that predict lift and rolling moment with sufficient accuracy for use in preliminary design.

Based upon the presented results it can be concluded that the nonlinear aerodynamic characteristics of slender wings can be predicted by the developed simple analytic relationships with better accuracy than through any other presently available theory.

Acknowledgment

The paper is based upon results obtained in a study made for NASA, Contract NASA 8-28310, under the direction of W. W. Clever, NASA MSFC, and J. C. Young, NASA JSC.

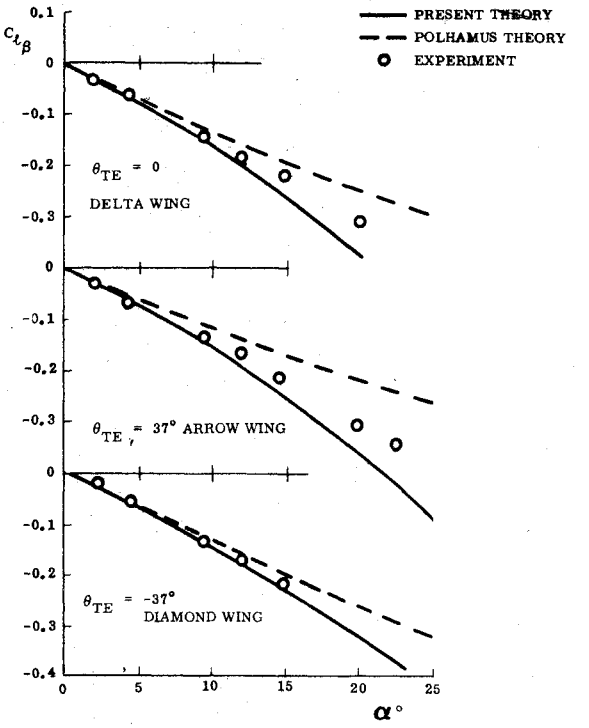

Fig. 12 Effect of trailing-edge sweep on lateral stability at $M_\infty = 0.8$.

References

[1] Ericsson, L. E. and Reding, J. P., "Analysis of Flow Separation Effects on the Dynamics of a Large Space Booster," *Journal of Spacecraft and Rockets*, Vol. 2, July-Aug. 1965, pp. 481-490.

[2] Rainey, A. G., "Progress on the Launch Vehicle Buffeting Problem," *Journal of Spacecraft and Rockets*, Vol. 2, May-June 1965, pp. 289-299.

[3] Ericsson, L. E. and Reding, J. P., "Unsteady Aerodynamics of Slender Delta Wings at Large Angles of Attack," *Journal of Aircraft*, Vol. 12, Sept. 1975, pp. 721-729.

[4] Polhamus, E. C., "Predictions of Vortex-Lift Characteristics by a Leading-Edge Suction Analogy," *Journal of Aircraft*, Vol. 8, April 1971, pp. 193-199.

[5] Jones, R. T., "Properties of Low-Aspect-Ratio Pointed Wings at Speeds Below and Above the Speed of Sound," NACA Rept. No. 835, May 1945.

[6] Peckham, O. H., "Low-Speed Wind-Tunnel Tests on a Series of Uncambered Slender Pointed Wings with Sharp Edges," Aeronautical Research Council, Great Britain, R&M 3186, Dec. 1958.

[7] Tosti, L. P., "Low Speed Static Stability and Damping-in-Roll Characteristics of Some Swept and Unswept Low-Aspect-Ratio Wings," NACA TN 1468, 1947.

[8] Fink, P. T., "Some Low Speed Experiments with 20-Degree Delta Wings," *Zeitschrift für Flugwissenschaften*, Vol. 4, July 1956, pp. 247-249.

[9] Earnshaw, P. B. and Lawford, J. A., "Low-Speed Wind-Tunnel Experiments on a Series of Sharp-Edged Delta Wings: Part 1, Forces, Moments, Normal-Force Fluctuations, and Position of Vortex Breakdown," Aeronautical Research Council, Great Britain, TN AERO 2780, Aug. 1961.

[10] Lawford, J. A. and Beauchamp, A. R., "Low-Speed Wind-Tunnel Measurements on A Thin Sharp-Edged Delta Wing with 70° Leading-Edge Sweep, with Particular Reference to Position of Leading-Edge-Vortex Breakdown," Aeronautical Research Council, Great Britain, R&M No. 3338, Nov. 1961.

[11] Bartlett, G. E. and Vidal, R. J., "Experimental Investigation of Influence of Edge Shape on the Aerodynamic Characteristics of Low Aspect Ratio Wings at Low Speeds," *Journal of the Aeronautical Sciences*, Vol. 22, Aug. 1955, pp. 517-533.

[12] Elle, B. J., "An Investigation at Low Speed of the Flow Near the Apex of Thin Delta Wings with Sharp Leading Edges," Aeronautical Research Council, Great Britain, R&M 3176, Jan. 1958.

[13] Gersten, K., "Nichtlineare Tragflächen Theorie insbesondere für Tragflügel mit kleinen Seitenverhältnis," *Ingenieur-Archiv.*, Vol. 30, 1961, pp. 431-452.

[14] Lamar, J. E., "Prediction for Vortex Flow Characteristics of Wings at Subsonic and Supersonic Speeds," *Journal of Aircraft*, Vol. 13, May 1976, pp. 490-494.

[15] Ville, G., "Influence des Decallements au Bord d'Attaque sur les Characteristiques Aerodynamiques des Voilures," *Association Francaise des Ingenieurs et Techniciens des l'Aeronautique et de l'Espace, Colloque d'Aerodynamique Appliquée*, 4th, Lille, France, Nov. 8-10, 1967.

[16] Ericsson, L. E. and Reding, J. P., "Stall Flutter Analysis," *Journal of Aircraft*, Vol. 10, Jan. 1973, pp. 5-13.

[17] Jacobs, E. N. and Sherman, A., "Airfoil Section Characteristics as Affected by Variations in the Reynolds Number," NACA TR 586, 1937.

[18] Hummel, D. and Srinivasan, P. S., "Vortex Breakdown Effects on the Low-Speed Aerodynamic Characteristics of Slender Delta Wings in Symmetrical Flow," *Journal of the Royal Aeronautical Society*, Vol. 71, April 1967, pp. 319-322.

[19] Reding, J. P. and Ericsson, L. E., "Delta Wing Separation Can Dominate Shuttle Dynamics," *Journal of Spacecraft and Rockets*, Vol. 10, July 1973, pp. 421-428.

[20] Woodgate, L., "Measurements of the Oscillatory Pitching Moment Derivatives on a Delta Wing with Round Leading Edges in Incompressible Flow," Aeronautical Research Council, Great Britain, R&M No. 3628, Pt. 1, July 1968.

[21] Ericsson, L. E. and Reding, J. P., "Dynamic Stall Analysis in Light of Recent Numerical and Experimental Results," *Journal of Aircraft*, Vol. 13, April 1976, pp. 248-255; see also AIAA Paper 75-26, Pasadena, Calf., Jan. 1975.

[22] Lambourne, N. C., Bryer, D. W., and Maybrey, J.F.M., "Pressure Measurements on a Model Delta Wing Undergoing Oscillatory Deformation," Aeronautical Research Council, Great Britain, NPL Aero Rept. 1314, March 1970.

[23] Davenport, E. E. and Huffman, J. K., "Experimental and Analytical Investigation of Subsonic Longitudinal and Lateral Aerodynamic Characteristics of Slender Sharp-Edge 74° Swept Wings," NASA TN D-6344, July 1971.

[24] Engler, P.B.E. and Moss, G. F., "Low-Speed Wind-Tunnel Tests on a 1/8th Scale Model of the Handley-Page HP 115," Aeronautical Research Council, Great Britain, R&M No. 3486, Aug. 1965.

[25] Hummel, D. and Redeker, G., "Über den Einfluss des Aufplatzens der Wirbel auf die aerodynamische Beiwerte von Deltaflügeln mit kleinen Seitenverhältnis beim Scheibeflug," *Jahrbuch der W.G.L.R.*, 1967, pp. 232-240.

[26] Hummel, D., "Untersuchungen über das Aufplatzen der Wirbel an schlanken Deltaflügeln," *Zeitschrift für Flugwissenschaften*, Vol. 13, May 1965, pp. 158-169.